Inorganic Chemistry
Article

Inorg. Chem. **2011**, *50*, 1743–1748 **1743**
DOI: 10.1021/ic102188v

Nanotubular Metal−Organic Frameworks with High Porosity Based on T-Shaped Pyridyl Dicarboxylate Ligands

Shenglin Xiang, Jing Huang, Lei Li, Jianyong Zhang,* Long Jiang, Xiaojun Kuang, and Cheng-Yong Su

School of Chemistry and Chemical Engineering, Sun Yat-Sen University, Guangzhou 510275, China.

Received October 30, 2010

Two nanotubular metal−organic frameworks (MOFs), $\{Cu(L1)\cdot 2H_2O\cdot 1.5DMF\}_\infty$ (**1**) and $\{Cu_2(L2)_2(H_2O)_2\cdot 7H_2O\cdot 3DMF\}_\infty$ (**2**), with novel topologies have been constructed based on Cu^{2+}, 5-(pyridin-4-yl)isophthalic acid (L1) and 5-(pyridin-3-yl)isophthalic acid (L2), respectively. Two MOFs were characterized by IR spectroscopy, thermogravimetry, single-crystal, and powder X-ray diffraction methods. Network analysis reveals a two-nodal (3,6)-connected $(4\cdot 6^2)_2(4^2\cdot 6^{10}\cdot 8^3)$ net and a three-nodal (3,4)-connected $(4\cdot 8^2)_4(4^2\cdot 8^2\cdot 10^2)_2(8^4\cdot 12^2)$ net. Interpenetration is inherently prevented by both of the topologies of the frameworks. The porosity of MOF **1** was confirmed by N_2 and CO_2 gas adsorption investigations. MOF **1** exhibits remarkable hydrogen sorption hysteresis at low pressure and a H_2 uptake capacity of 1.05 wt % at 77 K and 1 atm.

Introduction

Porous metal−organic frameworks (MOFs) have been studied intensively due to their potential application in gas storage, separation, and catalysis.[1] Incorporation of a paddlewheel $[M_2(RCOO)_4L_2]$ (M = Cu, Zn; L = axial ligand) motif has resulted in formation of highly porous paddlewheel frameworks, in which the axial ligand may be a solvent molecule or N-donor ligand. Paddlewheel-based MOFs are widely constructed by organic linkers with multiple carboxylate groups including a dicarboxylate linker,[2] tricarboxylate linker (e.g., 1,3,5-benzenetricarboxylic acid),[3] tetracarboxylate linker (e.g., 3,3′,5,5′-biphenyltetracarboxylic acid),[4] hexacarboxylate linker,[5] and so forth. Combined use of carboxylate ligands and diimines has resulted in a number of MOFs, for example, monocarboxylic acid and tripyridine[6] and monocarboxylic acid and tetrapyridine.[7] MOFs based on dicarboxylic acids and bridging diamines/diimines[8] have yielded interesting porous structures, whereas they are normally interpenetrated, thus reducing the porosity.[9]

*To whom correspondence should be addressed. E-mail: zhjyong@mail.sysu.edu.cn.

(1) Kitagawa, S.; Kitaura, R.; Noro, S. *Angew. Chem., Int. Ed.* **2004**, *43*, 2334–2375.

(2) (a) Furukawa, H.; Kim, J.; Ockwig, N. W.; O'Keeffe, M.; Yaghi, O. M. *J. Am. Chem. Soc.* **2008**, *130*, 11650–11661. (b) Burrows, A. D.; Frost, C. G.; Mahon, M. F.; Winsper, M.; Richardson, C.; Attfield, J. P.; Rodgers, J. A. *Dalton Trans.* **2008**, 6788–6795. (c) Bourne, S. A.; Lu, J.; Mondal, A.; Moulton, B.; Zaworotko, M. J. *Angew. Chem., Int. Ed.* **2001**, *40*, 2111–2113.

(3) (a) Chui, S. S. Y.; Lo, S. M. F.; Charmant, J. P. H.; Orpen, A. G.; Williams, I. D. *Science* **1999**, *283*, 1148–1150. (b) Ma, S.; Zhou, H. C. *J. Am. Chem. Soc.* **2006**, *128*, 11734–11735. (c) Sun, D.; Ma, S.; Ke, Y.; Collins, D. J.; Zhou, H. C. *J. Am. Chem. Soc.* **2006**, *128*, 3896–3897. (d) Ma, S.; Sun, D.; Ambrogio, M.; Fillinger, J. A.; Parkin, S.; Zhou, H. C. *J. Am. Chem. Soc.* **2007**, *129*, 1858–1859. (e) Yan, Y.; Lin, X.; Yang, S.; Blake, A. J.; Dailly, A.; Champness, N. R.; Hubberstey, P.; Schröder, M. *Chem. Commun.* **2009**, 1025–1027. (f) Zhao, X.; He, H.; Hu, T.; Dai, F.; Sun, D. *Inorg. Chem.* **2009**, *48*, 8057–8059.

(4) (a) Chen, B.; Ockwig, N. W.; Millward, A. R.; Contreras, D. S.; Yaghi, O. M. *Angew. Chem., Int. Ed.* **2005**, *44*, 4745–4749. (b) Lin, X.; Jia, J.; Zhao, X.; Thomas, K. M.; Blake, A. J.; Walker, G. S.; Champness, N. R.; Hubberstey, P.; Schröder, M. *Angew. Chem., Int. Ed.* **2006**, *45*, 7358–7364. (c) Wu, J. Y.; Yang, S. L.; Luo, T. T.; Liu, Y. H.; Cheng, Y. W.; Chen, Y. F.; Wen, Y. S.; Lin, L. G.; Lu, K. L. *Chem.—Eur. J.* **2008**, *14*, 7136–7139. (d) Wu, J. Y.; Ding, M. T.; Wen, Y. S.; Liu, Y. H.; Lu, K. L. *Chem.—Eur. J.* **2009**, *15*, 3604–3614. (e) Lin, X.; Telepeni, I.; Blake, A. J.; Dailly, A.; Brown, C. M.; Simmons, J. M.; Zoppi, M.; Walker, G. S.; Thomas, K. M.; Mays, T. J.; Hubberstey, P.; Champness, N. R.; Schröder, M. *J. Am. Chem. Soc.* **2009**, *131*, 2159–2171. (f) Wu, S.; Ma, L.; Long, L. S.; Zheng, L. S.; Lin, W. *Inorg. Chem.* **2009**, *48*, 2436–2442. (g) Ma, L.; Lee, J. Y.; Li, J.; Lin, W. *Inorg. Chem.* **2008**, *47*, 3955–3957.

(5) (a) Yan, Y.; Telepeni, I.; Yang, S.; Lin, X.; Kockelmann, W.; Daily, A.; Blake, A. J.; Lewis, W.; Walker, G. S.; Allan, D. R.; Barnett, S. A.; Champness, N. R.; Schröder, M. *J. Am. Chem. Soc.* **2010**, *132*, 4092–4094. (b) Zou, Y.; Park, M.; Hong, S.; Lah, M. S. *Chem. Commun.* **2008**, 2340–2342.

(6) (a) Batten, S. R.; Hoskins, B. F.; Moubaraki, B.; Murray, K. S.; Robson, R. *Chem. Commun.* **2000**, 1095–1096. (b) Liu, H. B.; Yu, S. Y.; Huang, H.; Zhang, Z. X. *Aust. J. Chem.* **2003**, *56*, 671–674.

(7) (a) Papaefstathiou, G. S.; MacGillivray, L. R. *Angew. Chem., Int. Ed.* **2002**, *41*, 2070–2073. (b) Ohmura, T.; Usuki, A.; Fukumori, K.; Ohta, T.; Ito, M.; Tatsumi, K. *Inorg. Chem.* **2006**, *45*, 7988–7990.

(8) (a) Chen, B.; Ma, S.; Zapata, F.; Fronczek, F. R.; Lobkovsky, E. B.; Zhou, H. C. *Inorg. Chem.* **2007**, *46*, 1233–1236. (b) Wen, Y. H.; Cheng, J. K.; Zhang, J.; Li, Z. J.; Kang, Y.; Yao, Y. G. *Inorg. Chem. Commun.* **2004**, *7*, 1120–1123. (c) Chen, B.; Fronczek, F. R.; Courtney, B. H.; Zapata, F. *Cryst. Growth Des.* **2006**, *6*, 825–828.

(9) Pichon, A.; Fierro, C. M.; Nieuwenhuyzen, M.; James, S. L. *CrystEngComm* **2007**, *9*, 449–451.

(10) For examples, see: (a) Pichon, A.; Lazuen-Garay, A.; James, S. L. *CrystEngComm* **2006**, *8*, 211–214. (b) Wei, Q.; Nieuwenhuyzen; James, S. L. *Microporous Mesoporous Mater.* **2004**, *73*, 97–100. (c) Xiong, R.-G.; Wilson, S. R.; Lin, W. B. *J. Chem. Soc., Dalton Trans.* **1998**, 4089–4090.

Published on Web 01/19/2011

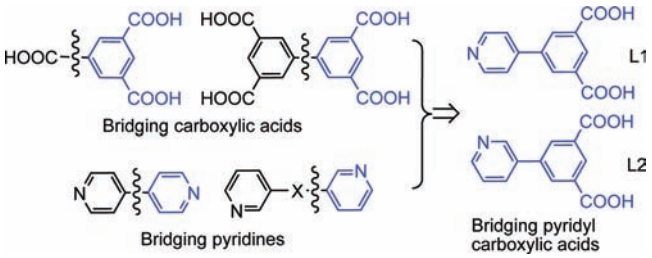

In contrast to plentiful research in bridging carboxylic acid or pyridyl ligands, it is surprising that little investigation of elongated bridging pyridyl carboxylic acids has been undertaken in MOFs. Known research is largely limited to truncated isonicotinic acid[10] and pyridinedicarboxylic acids,[11,12] with few exceptions.[13] Herein, we report two elongated pyridyl carboxylic acid ligands with one pyridyl donor and two carboxylic groups, namely, 5-(pyridin-4-yl)isophthalic acid (L1) and 5-(pyridin-3-yl)isophthalic acid (L2). On the basis of the T-shaped rigid ligands and the common paddlewheel $Cu_2(COO)_4$ motif, two MOFs have been synthesized, which are $\{Cu(L1)\cdot 2H_2O\cdot 1.5DMF\}_\infty$ (**1**) with 1D nanotubular channels and $\{Cu_2(L2)_2(H_2O)_2\cdot 7H_2O\cdot 3DMF\}_\infty$ (**2**) with interconnected tubular channels. They represent two novel topologies to inherently prevent interpenetration.

Results and Discussion

Syntheses and Crystal Structures. Solution reactions of $Cu(NO_3)_2\cdot 3H_2O$ with L1 in DMF-MeOH and of $Cu(OAc)_2\cdot H_2O$ with L2 in DMF-H_2O resulted in precipitates first, which were subsequently transformed to block crystals of **1** and **2**, respectively. Environmental temperature above 20 °C is preferred during the product formation.

Single-crystal X-ray diffraction reveals that $\{Cu(L1)\cdot 2H_2O\cdot 1.5DMF\}_\infty$ (**1**) crystallizes in monoclinic space group $P2_1/c$. The asymmetric unit consists of one copper ion and one L1 ligand (Figure 1). The central Cu(II) ion is five-coordinated by four oxygen atoms and one pyridyl N-donor (Cu−O 1.98−2.00 Å; Cu−N 2.15 Å) from five different L1 ligands in a square-pyramidal geometry. Four carboxylate groups from different ligands connect a pair of copper ions to generate the paddlewheel units (Cu···Cu distance of 2.68 Å), in which the axial positions are occupied by two pyridyl N-donors from another two different ligands. Considering the paddlewheel clusters as six-connecting nodes and the ligand L1 as three-connecting nodes, the overall structure of **1** is three-dimensional and topologically possesses a two-nodal (3,6)-connected net with stoichiometry $(3-c)_2(6-c)$. The point (Schläfli) symbol for **1** is $(4\cdot 6^2)_2(4^2\cdot 6^{10}\cdot 8^3)$ calculated with TOPOS.[14] Such a novel topological net with relatively high symmetry is rare, and the only example was reported by Davies et al.[15] Different from their negatively charged network with cations residing in the channels, the network of **1** is neutral.

There exist wide nanotubular channels with the L1 ligands serving as the walls, extending infinitely along the *a* axis. Adjacent tubular channels share the walls consisting of L1. The channels have a size of ~13.5 × 13.7 Å^2 ($b \times c$, $b \perp c$) along the diagonals of the quadrangle cross section. The pore width is ~6.2 Å if measured between the ligand channel walls, taking into consideration the van der Waals radius of carbon. The channels are filled by disordered H_2O and DMF solvent molecules in the as-prepared crystals of **1**. The solvent molecules are established to be two H_2O and 1.5 DMF molecules per Cu(L1) unit by elemental analysis and thermogravimetric analysis (TGA). The accessible volume is 54.0% (1088.9 Å^3) per unit cell (2015.9 Å^3), as estimated using PLATON.[16]

$\{Cu_2(L2)_2(H_2O)_2\cdot 7H_2O\cdot 3DMF\}_\infty$ (**2**) crystallizes in monoclinic space group $P2_1/c$. The asymmetric unit consists of two copper ions and two L2 ligands and two coordinated H_2O molecules. As shown in Figure 2a, there are two crystallographically unique Cu(II) ions. The Cu1 ion is five-coordinated in a square-pyramidal geometry with a N_2O_3 donor set. The equatorial plane is occupied by two N-donors and two O-donors from different L2 ligands (Cu1−O 1.93−1.95 Å; Cu1−N 2.06−2.07 Å), and the axial position is completed by one coordinated H_2O molecule (Cu2−O 2.21 Å). The Cu2 ion is five-coordinated with four O-donors from different L2 ligands and one coordinated H_2O molecules (Cu2−O 1.95−1.96 Å; Cu2−O_w 2.15 Å). A pair of Cu2 ions is bridged by four carboxylate groups from four different L2 ligands to form a paddlewheel unit. Such a tendency for Cu(II) to exhibit multiple coordination geometries was observed previously by Zaworotko et al.[17] Four Cu1 and two Cu2 paddlewheel units are connected by four L2 ligands to form a tubular secondary building units (SBUs) (Figure 2b,c). The tubular cavities have a size of ~14.1 × 14.6 Å^2 ($b \times c$) along the diagonals of the quadrangle cross section. The 3D framework can be considered to consist of the tubular SBUs. Every two tubular SBUs are connected via sharing a Cu2 paddlewheel unit in the *ab* plane, and each SBU is linked with other four SBUs via Cu1 in the *bc* plane (Figure 2d,e).

(11) For the MOF examples based on 3,5-pyridinedicarboxylic acid, see: (a) Eubank, J. F.; Walsh, R. D.; Eddaoudi, M. *Chem. Commun.* **2005**, 2095–2097. (b) Wang, P.; Moorefield, C. N.; Panzner, M.; Newkome, G. R. *Cryst. Growth Des.* **2006**, *6*, 1563–1565. (c) Lu, Y. L.; Wu, J. Y.; Chan, M. C.; Huang, S. M.; Lin, C. S.; Chiu, T. W.; Liu, Y. H.; Wen, Y. S.; Ueng, C. H.; Chin, T. M.; Hung, C. H.; Lu, K. L. *Inorg. Chem.* **2006**, *45*, 2430–2437. (d) Jia, J.; Lin, X.; Blake, A. J.; Champness, N. R.; Hubberstey, P.; Shao, L.; Walker, G.; Wilson, C.; Schröder, M. *Inorg. Chem.* **2006**, *45*, 8838–8840. (e) Wang, D. E; Tian, Z. F.; Wang, F.; Wen, L. L.; Li, D. F. *J. Inorg. Organomet Polym.* **2009**, *19*, 196–201. (f) Hafizović, J.; Krivokapić, A.; Szeto, K. C.; Jakobsen, S.; Lillerud, K. P.; Olsbye, U.; Tilset, M. *Cryst. Growth Des.* **2007**, *7*, 2302–2304. (g) Burrows, A. D.; Mahon, M. F.; Wong, C. T. F. *CrystEngComm* **2008**, *10*, 487–489.

(12) For the MOF examples based on 2,3-, 2,4-, or 2,5-pyridinedicarboxylic acids, see: (a) Mahata, P.; Sankar, G.; Madras, G.; Natarajan, S. *Chem. Commun.* **2005**, 5787–5789. (b) Noro, S.; Miyasaka, H.; Kitagawa, S.; Wada, T.; Okubo, T.; Yamashita, M.; Mitani, T. *Inorg. Chem.* **2005**, *44*, 133–146. (c) Soares-Santos, P. C. R.; Cunha-Silva, L.; Paz, F. A. A.; Ferreira, R. A. S.; Rocha, J.; Trindade, T.; Carlos, L. D.; Nogueira, H. I. S. *Cryst. Growth Des.* **2008**, *8*, 2505–2516. (d) Liu, Y.; Kravtsov, V. Ch.; Beauchamp, D. A.; Eubank, J. F.; Eddaoudi, M. *J. Am. Chem. Soc.* **2005**, *127*, 7266–7267.

(13) Yang, W.; Lin, X.; Jia, J.; Blake, A. J.; Wilson, C.; Hubberstey, P.; Champness, N. R.; Schröder, M. *Chem. Commun.* **2008**, 359–361.

(14) Blatov, V. A.; Peaskov, M. V. *Acta Crystallogr., Sect. B* **2006**, *62*, 457–466.

(15) Davies, K.; Bourne, S. A.; Öhrström, L.; Oliver, C. L. *Dalton Trans.* **2010**, *39*, 2869–2874.

(16) Spek, A. L. *J. Appl. Crystallogr.* **2003**, *36*, 7–13.

(17) McManus, G. J.; Wang, Z.; Beauchamp, D. A.; Zaworotko, M. J. *Chem. Commun.* **2007**, 5212–5213.

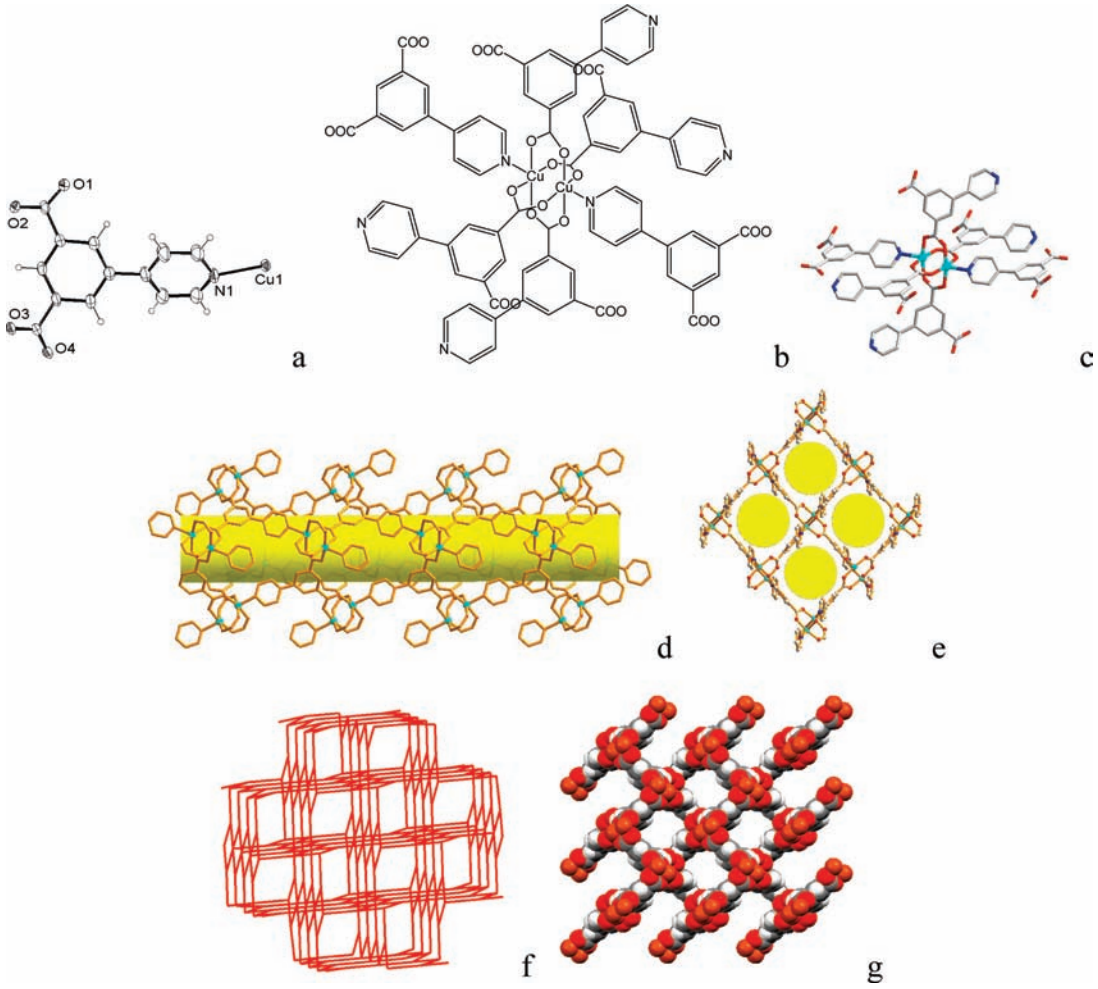

Figure 1. (a) ORTEP diagram showing the asymmetric unit of **1** by thermal vibration ellipsoids with a 30% probability level. (b) Molecular structure drawing and (c) molecular structure of the paddlewheel copper unit (six-connected node). (d) One tubular channel along the *a* axis. (e) Tubular channels perpendicular to the *bc* plane of **1**. (f) $(4\cdot6^2)_2(4^2\cdot6^{10}\cdot8^3)$ topological diagram. (g) Space-filling representation of **1** along the *a* axis.

If the Cu1 ions and Cu2 paddlewheel clusters are simplified as four-connecting nodes and the ligand is simplified as a three-connecting node, the net topological analysis of **2** reveals an undocumented less-symmetric three-nodal (3,4)-connected net with stoichiometry $(3-c)_4(4-c)_3$ (Figure 2f). The point (Schläfli) symbol for **2** is $(4\cdot8^2)_4$-$(4^2\cdot8^2\cdot10^2)_2(8^4\cdot12^2)$. The framework creates interconnected channels which extend along *c* and *a* axes (Figure 2g,h). The tubular SBUs are arranged along the *c* axis in a zigzag manner, while the individual SBU tubular cavities are disrupted by the channel along the *a* axis. The channels along the *a* axis have an irregular shape created by packing of tubular SBUs. Disordered DMF and H_2O solvent molecules are located in the interconnected channels. The solvent molecules were established to be three DMF and seven H_2O solvent molecules per $Cu_2(L2)_2$-$(H_2O)_2$ formula unit determined by elemental analysis and TGA. **2** possesses a larger solvent-accessible volume of 60.6% (3145.0 $Å^3$) per unit cell (5186.0 $Å^3$) calculated using PLATON. However, the disordered guest molecules may play a key role in stabilizing the host framework via weak interactions (see below).

X-ray power diffraction (XRPD) was used to confirm the phase purity of **1** (Figure 3a,b) and **2** (Figure 3e,f). The patterns for the as-synthesized bulk products closely match the simulated ones from the single-crystal analysis, which are indicative of the pure solid-state phases.

Thermogravimetric Analyses. TGA shows that **1** is stable up to 300 °C. The weight loss of 31.6% from RT to 260 °C corresponds to the loss of two guest DMF and two uncoordinated water molecules per Cu(L1) unit (calcd: 32.3%). There is no weight loss from 260 to 300 °C. Complex **2** has a higher weight loss of 38.5% upon heating from RT to 200 °C, which is attributed to the loss of three guest DMF and nine solvated/coordinated water molecules per $Cu_2(L2)_2$ (calcd: 39.1%). The frameworks of **1** and **2** may be anticipated to collapse above 300 and 290 °C, respectively (Figure 4).

Gas Sorption. To study the porosity of **1** and **2**, nitrogen physisorption measurements was preformed at 77 K. For this purpose, the synthesized materials were dried to remove the guest molecules by evacuation under a dynamic vacuum at 90 °C for 10 h. TGA shows that the solvent was removed completely for **1** (Figure 4c). The XRPD pattern

(18) No crystal suitable for single-crystal X-ray diffraction analysis was obtained, and no suitable structural model could be established based on the XRPD, which prevented us from getting further structural information of the guest-free state.

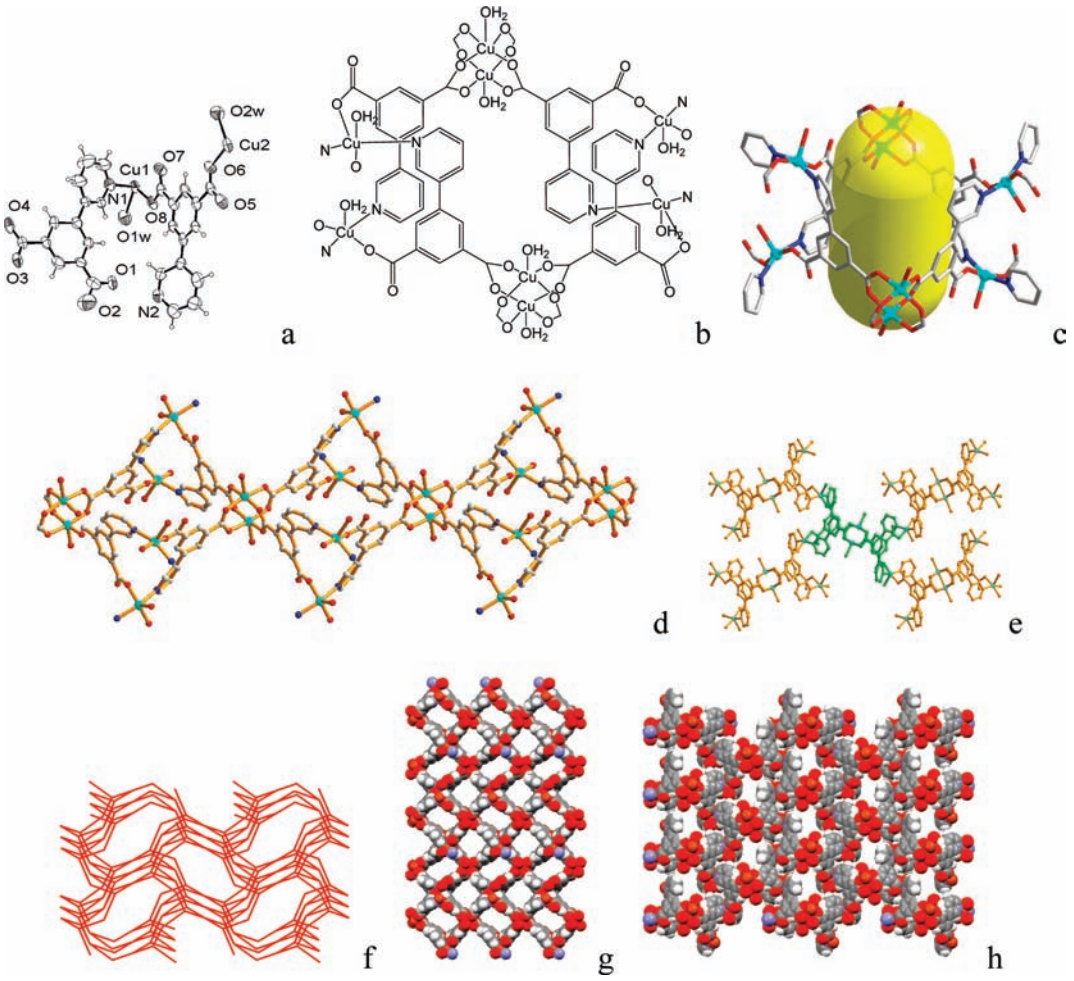

Figure 2. (a) ORTEP diagram showing the asymmetric unit of **2** by thermal vibration ellipsoids with a 30% probability level. (b) Molecular structure drawing and (c) molecular structure of tubular SBU formed by four L2 ligands linked by eight Cu ions. (d) Connectivity of tubular SBUs in the *ab* plane of **2**. (e) Connectivity of tubular SBUs in the *bc* plane. For clarity, the one-tubular SBU is shown in green. (f) $(4\cdot8^2)_4(4^2\cdot8^2\cdot10^2)_2(8^4\cdot12^2)$ topological diagram. Space-filling representation of **2** along the *c* axis (g) and along the *a* axis (h).

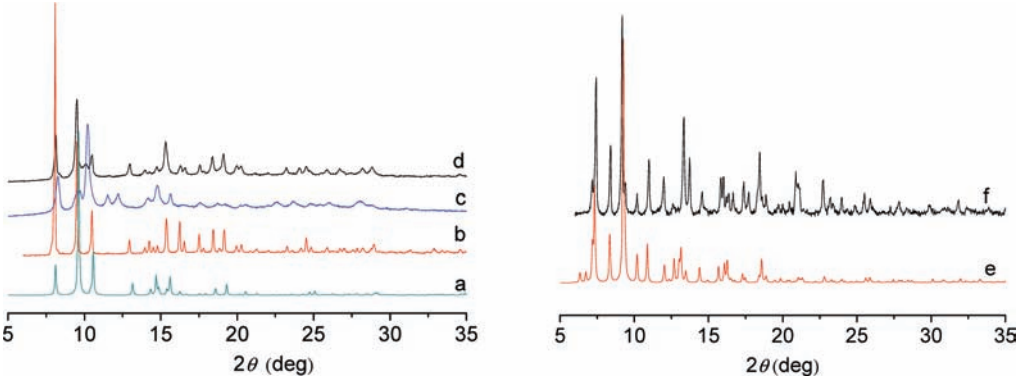

Figure 3. Comparison of XRPD patterns of **1** and **2**; (a) **1** simulated patterns from the single-crystal structure determination, (b) **1** as-synthesized products, (c) guest-free **1**, (d) guest-free **1** after dipping in the mother liquor for 1 day, (e) **2** simulated patterns from the single-crystal structure determination, and (f) **2** as-synthesized products.

of guest-free **1** confirms the stability of the framework in the absence of guest molecules, characteristic of peak broadening and peak shifts at higher 2θ angles probably related to the conformational change of the ligand (Figure 3c).[18] The XRPD peaks could reversibly sharpen and shift back as the sample gets resolvated in the mother liquor (Figure 3d). The nitrogen physisorption measurement reveals that **1** exhibits a type-I isotherm, indicative of microporous materials (Figure 5a). The nitrogen adsorption shows good reversibility. **1** has a total pore volume of 0.28 $cm^3\ g^{-1}$. The Langmuir and Brunauer–Emmett–Teller (BET) surface areas are 719 and 431 $m^2\ g^{-1}$, respectively, derived from the adsorption data. In contrast, the guest removal of **2** under similar conditions causes a loss in crystallinity and leads to the gas sorption behavior of nonporous materials.

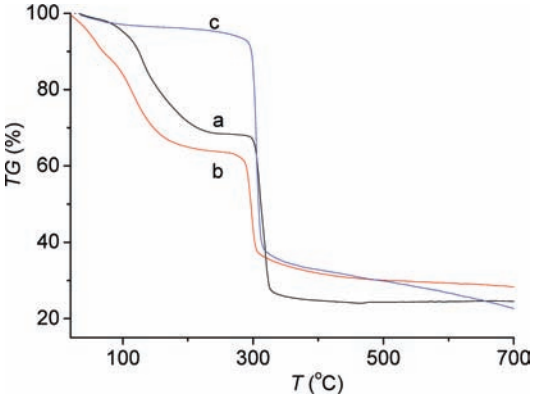

Figure 4. TGA curves of **1** and **2** recorded under a N_2 atmosphere; (a) **1** as-synthesized, (b) **2** as-synthesized, and (c) **1** after the removal of guest molecules.

Adsorption of carbon dioxide and hydrogen by guest-free **1** was also studied. Carbon dioxide sorption at 195 K gave a reversible type-I isotherm (Figure 5b). The uptake at 1 atm (1 atm = 101 325 Pa) reached 118 $cm^3\ g^{-1}$ (5.27 mmol g^{-1}), which amounts to 17.3 CO_2 molecules per formula unit. The hydrogen adsorption isotherm indicates an uptake of 117 $cm^3\ g^{-1}$ (~1.05 wt %) at 77 K and 1 atm (Figure 5c). In contrast to the nitrogen and carbon dioxide sorption isotherms, the hydrogen sorption isotherm displays remarkable hysteresis between adsorption and desorption curves at 77 K. The hysteretic desorption indicates strong interaction between H_2 and host frameworks and allows H_2 to be adsorbed at high pressures but stored at lower pressures, which has been reported recently in a few examples.[19−22] Considering the absence of vacant metal coordination sites[19] and kinetic traps[20] within the framework of **1**, the present hydrogen sorption hysteresis is possibly related to the presence of narrow pores (~6.2 Å)[21] and tubular channels.[22] An optimal pore size of just slightly over twice the kinetic diameter of the hydrogen molecules (about 6 Å) strengthens the interactions between H_2 molecules and pore walls.[23] The strong interactions between H_2 and the host framework are reflected by the high value of the isosteric heat of adsorption (Q_{st}), which was calculated to be 8.4−9.2 kJ mol^{-1} utilizing the Clausius−Clapeyron equation using isotherms measured at 77 and 87 K.[23b]

(19) Forster, P. M.; Eckert, J.; Heiken, B. D.; Parise, J. B.; Yoon, J. W.; Jhung, S. H.; Chang, J.-S.; Cheetham, A. K. *J. Am. Chem. Soc.* **2006**, *128*, 16846–16850.

(20) (a) Yang, S.; Lin, X.; Blake, A. J.; Walker, G. S.; Hubberstey, P.; Champness, N. R.; Schröder, M. *Nat. Chem.* **2009**, *1*, 487–493. (b) Zhao, X.; Biao, Bo.; Fletcher, A. J.; Thomas, K. M.; Bradshaw, D.; Rosseinsky, M. J. *Science* **2004**, *306*, 1012–1015. (c) Choi, H. J.; Dincă, M.; Long, J. R. *J. Am. Chem. Soc.* **2008**, *130*, 7848–7850. (d) Chen, B.; Ma, S.; Hurtado, E. J.; Lobkovsky, E. B.; Zhou, H.-C. *Inorg. Chem.* **2007**, *46*, 8490–8492. (e) Ma, S.; Wang, X.-S.; Manis, E. S.; Collier, C. D.; Zhou, H.-C. *Inorg. Chem.* **2007**, *46*, 3432–3434. (f) Férey, G.; Latroche, M.; Serre, C.; Millange, F.; Loiseau, T.; Percheron-Guégan, A. *Chem. Commun.* **2003**, 2976–2977.

(21) Chun, H.; Dybtsev, D. N.; Kim, H.; Kim, K. *Chem.—Eur. J.* **2005**, *11*, 3521–3529.

(22) Guo, Z.; Li, G.; Zhou, L.; Su, S.; Lei, Y.; Dang, S.; Zhang, H. *Inorg. Chem.* **2009**, *48*, 8069–8071.

(23) (a) Luo, J.; Xu, H.; Liu, Y.; Zhao, Y.; Daemen, L. L.; Brown, C.; Timofeeva, T. V.; Ma, S.; Zhou, H.-C. *J. Am. Chem. Soc.* **2008**, *130*, 9626–9627. (b) Barman, S.; Furukawa, H.; Blacque, O.; Venkatesan, K.; Yaghi, O. M.; Berke, H. *Chem. Commun.* **2011**, *46*, 7981–7983. (c) Chen, B.; Zhao, X.; Putkham, A.; Hong, K.; Lobkovsky, E. B.; Hurtado, E. J.; Fletcher, A. J.; Thomas, K. M. *J. Am. Chem. Soc.* **2008**, *130*, 6411–6423.

Conclusion

In summary, on the basis of T-shaped pyridyl dicarboxylate linkers and Cu^{2+}, two highly porous nanotubular MOFs with novel topologies have been synthesized and characterized. Both of the topologies inherently prevent interpenetration, and the frameworks possess large solvent-accessible volumes. It suggests that a combination of carboxylate and pyridyl groups in a T-shaped ligand may yield nanotubular MOFs with borderline transition-metal ions. It represents a new strategy to build nanotubular structures.[24] N_2 and CO_2 gas adsorption investigations show that MOF **1** is highly porous, and the remarkable hydrogen sorption hysteresis at low pressure and a H_2 uptake capacity of 1.05 wt % at 77 K and 1 atm suggest that nanotubular MOFs are promising materials for gas storage.

Experimental Section

Materials and Methods. All starting materials and solvents were obtained from commercial sources and used without further purification. 4-(3,5-Dimethylphenyl)pyridine and 3-(3,5-dimethylphenyl)pyridine were prepared according to published procedures.[25] X-ray power diffraction data were recorded on a Bruker D8 Advance diffractometer at 40 kV and 40 mA with a Cu-target tube and a graphite monochromator. Infrared spectra were measured on a Nicolet/Nexus-670 FT-IR spectrometer with KBr pellets. Thermogravimetric analysis was performed under N_2 at a heating rate of 10 °C/min on a Netzsch Thermo Microbalance TG 209 F3 Tarsus. The sorption isotherms for N_2 (77 K), H_2 (77 K), and CO_2 (195 K) gas were measured with a BELSORP-max automatic volumetric sorption apparatus.

5-(Pyridin-3-yl)isophthalic Acid (L2). To a solution of 3-(3,5-dimethylphenyl)pyridine (0.75 g, 4.1 mmol) in water/*tert*-butyl alcohol (v:v = 1:1, 20 mL), $KMnO_4$ (5.8 g) was added in 10 portions at 80 °C during a period of 24 h. After the last charge, the purple color of $KMnO_4$ did not fade. A solution of $Na_2S_2O_3$ (~2 mol L^{-1}) was added to the hot mixture until the purple color disappeared. The mixture was filtered by suction, and the residue was washed with water. The filtrate was acidified by H_2SO_4 (1 mol L^{-1}) to pH ≈ 5. The white precipitate was filtered and dried (0.52 g, 52%). ^{1}H NMR (300 MHz, DMSO-d_6, δ): 8.92 (s, 1H), 8.62 (s, 1H), 8.48 (s, 1H), 8.39 (s, 2H),8.12 (d, 1H, $^3J_{H-H}$ = 7.8 Hz); 7.52 (m, 1H).

5-(Pyridin-4-yl)isophthalic Acid (L1). L1 was prepared using a procedure analogous to that described for L2, replacing 3-(3,5-dimethylphenyl)pyridine with 4-(3,5-dimethylphenyl)pyridine, affording the desired product (75%). ^{1}H NMR (300 MHz, DMSO-d_6, δ): 8.7 (d, $^3J_{H-H}$ = 5.4 Hz, 2H), 8.51(s, 1H), 8.45 (s, 2H), 7.8 (d, 2H; $^3J_{H-H}$ = 6.0 Hz).

Synthesis of $\{Cu(L1)\cdot 2H_2O\cdot 1.5DMF\}_\infty$ (1). A buffer layer of DMF-MeOH (v:v = 1:1, 2 mL) was carefully layered over a solution of L1 (12.7 mg, 0.05 mmol) in DMF (2 mL). Then, a solution of $Cu(NO_3)_2\cdot 3H_2O$ (12.1 mg, 0.05 mmol) in MeOH (2 mL) was layered over the buffer layer. The solution was left to stand at RT, and green block crystals appeared after about 4 days (19 mg, 84%). Elemental analysis: found (calc.) for $C_{17.5}H_{21.5}CuN_{2.5}O_{7.5}$ (450.416): C 46.58 (46.67), H 4.53 (4.81), N 7.73 (7.77)%. IR (cm^{-1}, KBr): 3433s, 2926m, 1673s,1620vs, 1507m, 1441m, 1383vs, 1299 m, 1256w, 1223w, 1087m, 836w, 777m, 725m, 647w, 566w, 477w.

Synthesis of $\{Cu_2(L2)_2(H_2O)_2\cdot 7H_2O\cdot 3DMF\}_\infty$ (2). A solution of L2 (12.7 mg, 0.05 mmol) in DMF (2 mL) was mixed with a solution of $Cu(OAc)_2\cdot H_2O$ (10.0 mg, 0.05 mmol) in DMF-H_2O (v:v = 1:1, 2 mL), resulting in formation of a blue precipitate

(24) Ma, S.; Simmons, J. M.; Yuan, D.; Li, J.-R.; Weng, W.; Liu, D.-J.; Zhou, H.-C. *Chem. Commun.* **2007**, 4049–4051, and references therein.

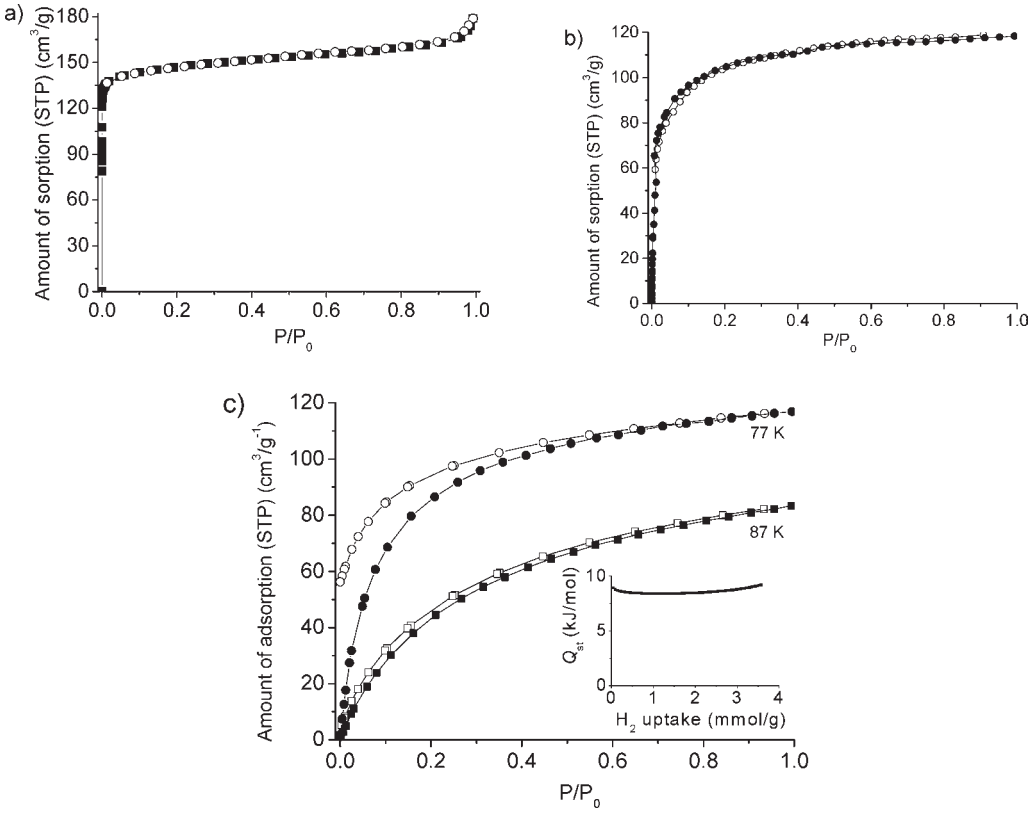

Figure 5. (a) Nitrogen adsorption−desorption isotherm of **1** at 77 K. (b) Carbon dioxide adsorption−desorption isotherm of **1** at 195 K. (c) Hydrogen adsorption−desorption isotherm of **1** at 77 and 87 K, showing pronounced hysteresis upon desorption at 77 K. Inset: the coverage dependencies of adsorption enthalpies of hydrogen. Filled and open circles denote adsorption and desorption, respectively.

immediately. The blue precipitate was subsequently transformed to blue block crystals after about 2 days (20 mg, 90%). Elemental analysis: found (calc.) for $C_{35}H_{53}Cu_2N_5O_{19}$ (974.918): C 43.00 (43.12), H 5.10 (5.48), N 6.89 (7.18)%. IR (cm^{-1}, KBr): 3417vs, 2926m, 1655vs, 1621vs, 1571s, 1487m, 1450m, 1411s, 1384vs, 1365vs, 1301m, 1198w, 1101m, 1061m, 776m, 657m, 610w, 567w, 488w, 468w.

X-ray Structure Determination. X-ray crystallographic intensity data were collected for **1** and **2** using an Oxford Gemini S Ultra diffractometer equipped with a graphite monochromated Enhance (Cu) X-ray source (λ = 1.54178 Å). The structures were solved by the direct methods following difference Fourier syntheses and refined by the full-matrix least-squares method against F_0^2 using SHELXTL software.[26] All non-hydrogen atoms were refined with anisotropic thermal parameters, while the hydrogen atoms on the ligands were placed in idealized positions with isotropic thermal parameters. The hydrogen atoms of the coordination water molecules could not be located but are included in the formulas. In complex **2**, one carboxylate oxygen atom is distributed over two sites (O2 and O2′). Because guest solvent molecules were highly disordered and impossible to refine using conventional discrete-atom models, the SQUEEZE subroutine of the PLATON software suite[27] was applied to remove the scattering from the highly disordered solvent molecules, and sets of solvent-free diffraction intensities were produced. The final formula was calculated from the SQUEEZE results, TGA, and elemental analysis.

Crystallographic data for **1**: $C_{17.5}H_{21.5}CuN_{2.5}O_{7.5}$: FW = 450.41, monoclinic, $P2(1)/c$, a = 11.9132(10) Å, b = 13.5460(11) Å, c = 13.6700(15) Å, α = 90°, β = 113.959(11)°, γ = 90°, V = 2015.9(3) Å^3, Z = 4, T = 150(2) K, λ = 1.54178 Å, μ = 1.939 mm^{-1}, 5212 reflections were collected (3121 were unique) for 4.06 < θ < 62.65, R(int) = 0.0658, R_1 = 0.1104, wR_2 = 0.2398 [$I > 2\sigma(I)$], R_1 = 0.1401, wR_2 = 0.2482 (all data) for 172 parameters, GOF = 1.087. CCDC-774764.

Crystallographic Data for **2**: $C_{35}H_{55}Cu_2N_5O_{20}$: FW = 992.92, monoclinic, $P2(1)/c$, a = 14.564(3) Å, b = 26.220(5) Å, c = 14.207(5) Å, α = 90°, β = 107.08(3)°, γ = 90°, V = 5186(2) Å^3, Z = 4, T = 150(2) K, λ = 1.54178 Å, μ = 1.625 mm^{-1}, 27152 reflections were collected (7955 were unique) for 3.17 < θ < 63.00, R(int) = 0.1014, R_1 = 0.0857, wR_2 = 0.2008 [$I > 2\sigma(I)$], R_1 = 0.1437, wR_2 = 0.2145 (all data) for 371 parameters, GOF = 0.896. CCDC-774765.

Acknowledgment. We gratefully acknowledge the Natural Science Foundation of China (Grant No. 20903121), the Specialized Research Fund for the Doctoral Program of Higher Education of China, the Fundamental Research Funds for the Central Universities, and the SRF for ROCS of SEM for support.

Supporting Information Available: Crystal and structure refinement data and IR spectra. This material is available free of charge via the Internet at http://pubs.acs.org.

(25) Huang, J.; He, L.; Zhang, J.; Chen, L.; Su, C.-Y. *J. Mol. Catal. A: Chem.* **2010**, *317*, 97–103.
(26) Sheldrick, G. M. *SHELX-97: Program for Crystal Structure Solution and Refinement*; University of Götingen, Götingen, Germany, 1997.
(27) Spek, A. L. *Acta Crystallogr., Sect. A* **1990**, *46*, C34.